Organic electro-optic materials combining extraordinary nonlinearity with exceptional stability to enable commercial applications

Scott R. Hammond*[a,b], Kevin M. O'Malley[a], Huajun Xu[b], Delwin L. Elder[a,b], Lewis E. Johnson[a,b]
[a]Nonlinear Materials Corporation, 2212 Queen Anne Ave North Box #324, Seattle, WA, USA 98109-2383
[b]Dept. of Chemistry, University of Washington, 4000 15th Ave NE, Seattle, WA USA 98195-0008
*Corresponding author: scotth@nonlinearmaterials.com

ABSTRACT

Hybrid organic electro-optic (OEO) modulators consist of a layer of ordered organic chromophores confined between layers of metals or semiconductors, enabling optical fields to be tightly confined within the OEO material. The combination of tight confinement with the high electro-optic (EO) performance of state-of-the-art OEO materials enables extraordinary EO modulation performance in silicon-organic hybrid (SOH) and plasmonic-organic hybrid (POH) device architectures. Recent records in POH devices include bandwidths >500 GHz and energy efficiency <100 aJ/bit. To enable commercial applications of these materials and devices, however, they must withstand demanding thermal and environmental conditions, both during manufacture and operation. To address these concerns, we examined the long-term thermal and environmental shelf storage stability of state-of-the-art commercial and developmental OEO materials under a variety of conditions relevant to Telecordia GR-468-CORE standards. We examined the shelf storage of poled OEO materials under a nitrogen atmosphere at a range of temperatures from 85 ˚C up to 150 ˚C to understand the kinetics of the thermally activated de-poling of the OEO materials. We also examined the shelf storage of OEO materials under a variety of atmospheres, including the aggressive 85 ˚C and 85% relative humidity damp heat condition, to understand the relative sensitivities of the materials to water and oxygen at different temperatures. We analyze the results of these studies and discuss their implications for commercial application of these materials and devices, including manufacturing, encapsulation requirements, and expected operational lifetimes.

Keywords: organic electro-optic, nonlinear optical polymer, organic-inorganic hybrid devices, thermal stability, environmental stability, Telecordia

1. INTRODUCTION

Organic electro-optic (OEO) materials have long been a subject of active R&D and potential commercial interest due to the ultra-fast (femtosecond) response time of their Pockels effect: a linear shift in refractive index with applied electric field.[1-3] The ultrafast response time is due to requiring only a shift in electron density in the π-electron system of the organic chromophores that make up OEO materials, whereas competing inorganic materials such as lithium niobate ($LiNbO_3$) require atomic displacement.[2] Furthermore, while the electro-optic coefficient (r_{33}) of $LiNbO_3$ and related materials are fixed by nature, the r_{33} of OEO materials can be continually improved through organic synthesis and materials development; indeed new records in excess of 1000 pm/V at 1310 nm have recently been demonstrated.[4, 5]

OEO materials have recently seen a renaissance due to the development of hybrid OEO device architectures,[6] where the organic material is confined on the nanoscale between either semiconductors or plasmonic metals, tightly confining the optical mode within the OEO material and maximizing the electro-optic (EO) effect. Such hybrid architectures have enabled extraordinary EO modulator performance in silicon-organic hybrid (SOH)[7-9] and plasmonic-organic hybrid (POH)[10-13] devices, as well as proof-of-concept demonstration in III-V semiconductors such as indium phosphide.[14] Highlights include (Figure 1) a POH Mach-Zehnder modulator (MZM) with >500 Ghz bandwidth,[15] a POH IQ modulator with <100 aJ/bit energy efficiency,[16] monolithic integration of a POH modulator with BiCMOS electronics demonstrating stable operation under demanding thermal conditions,[17] and compact, low-loss, high-performance SOH modulators implemented on silicon photonics platforms.[7, 9] These results have attracted considerable commercial interest due to the need for high-bandwidth, compact, power-efficient modulators for photonic

integrated circuits (PICs), with potential applications ranging from optical interconnects for datacom to microwave photonics, mmWave telecom, satellite communications, ultra-high performance metrology, and a wide variety of defense-related technologies. To enable commercial applications of OEO materials and devices, however, they must withstand demanding thermal and environmental conditions, both during manufacture and operation.

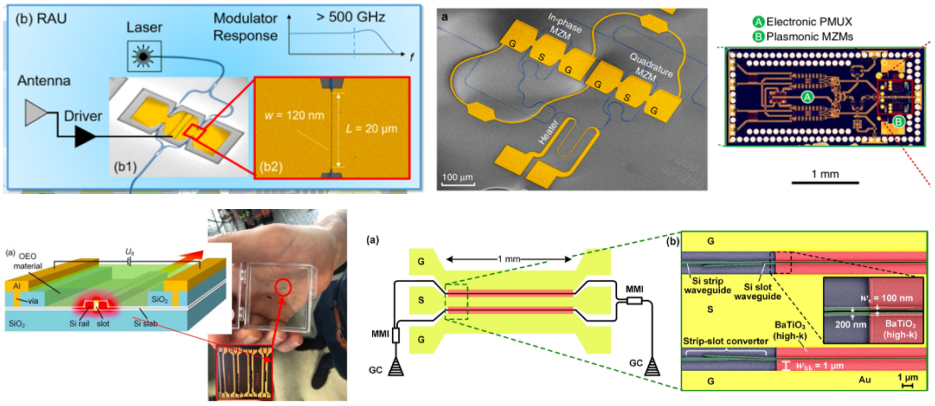

Figure 1. Highlights of recent hybrid OEO devices, including a >500 GHz bandwidth POH MZM (upper left),[15] a sub 100 aJ/bit POH IQ modulator (upper center),[16] a >100 Gbit/s integrated POH-SiGe BiCMOS transmitter (upper right),[17] a low-voltage sub-mm SOH MZM (lower left),[7] and a >76 GHz capacitively coupled SOH MZM (lower right).[9]

To enable commercial development of hybrid OEO devices, sufficient stability of OEO materials—which has long been a subject of concern—must be demonstrated. While, ultimately, stability of hybrid OEO devices under operation must be proved to enable commercial offerings, an interim step of demonstrating material stability under conditions specified in the Telecordia GR-468-CORE standards should give high confidence to device manufacturers to proceed with development of OEO devices. Organic optoelectronic materials did not initially have a good reputation for stability. Yet through creative engineering, even highly sensitive organic and hybrid materials have been successfully commercialized in OLEDs, as well as other technologies. Based on our results, OEO materials are substantially less sensitive than those used in OLEDs, and hence expensive ultra-barriers (such as used in OLEDs) and hermetic chip sealing technologies may not be required in all cases.

2. DESCRIPTION OF MATERIALS

OEO materials are comprised of highly dipolar chromophores. The molecules are composed of an electron rich donor connected via a π-conjugated bridge to an electron poor acceptor, creating an asymmetric potential energy well for electron density to be manipulated in. This molecular asymmetry is required for second-order nonlinear processes to be non-zero. Driven by theory-aided design, these chromophores have been engineered to optimize the asymmetry and exhibit exceptionally large hyperpolarizabilities (β), and consequently exhibit very large dipole moments (μ) as well.[1, 11] These chromophores must also be arranged non-centrosymmetrically in bulk (films) to achieve the net asymmetry required for second-order nonlinear processes, such as the Pockels effect. This is generally accomplished via electric field poling, where the OEO material is heated up above its glass transition temperature (T_g) to enable local molecular motion, and a large electric poling field (~100 V/μm) is applied and the dipolar chromophores reorient to align with this field, then the material is cooled down below T_g to lock the induced acentric order in place. The average degree of acentric order achieved, described by $\langle\cos^3\theta\rangle$, where θ is the angle between the molecular dipole moment and the poling field, is directly proportional to the electro-optic coefficient r_{33}, as described by:

$$r_{33} = G(n,\varepsilon,\omega)\beta_{zzz}\rho_N\langle\cos^3\theta\rangle \qquad (1)$$

The G term describes local-field factors that depend on the wavelength of light and the dielectric response of the material, including a factor of $2/n_\omega^4$, β_{zzz} describes the component of the hyperpolarizability tensor along the dipolar axis, and ρ_N describes the number density of the chromophores. [2, 11, 18]

Traditionally, chromophores were dispersed in a host polymer, such as PMMA or amorphous polycarbonate, at relatively low concentrations (~20-30 wt.%), such that the T_g of the host polymer dictated the thermal stability of the composite OEO materials. In such systems, the chromophores began reorienting to the thermodynamically stable centrosymmetric alignment, as demonstrated by a reduction in r_{33}, as much as 20-30 ˚C below the T_g of the host material,[19, 20] resulting in relatively poor thermal stability.[21] Chromophores have also been grafted onto polymer side-chains in an attempt to improve thermal stability, with similar overall results.[2] By replacing the polymer hosts with very high T_g materials, thermal stability of OEO materials has been improved,[22, 23] yet even these materials still show significant initial thermal relaxation of the r_{33} at moderate temperatures (~ 85 ˚C) before a steady state has been achieved. Furthermore, guest-host and side-chain polymer systems generally have relatively low chromophore concentrations, as increasing the concentration further usually leads to reduced poling efficiency as well as loss of the high T_g properties of the host, limiting the peak r_{33} achievable. One method to circumvent these issues is to use chromophores and/or polymer hosts that can undergo crosslinking reactions to increase the T_g during poling.

Recently, a new class of OEO materials (HLD chromophore) has been developed consisting of a binary chromophore system where each chromophore is appended with one complementary component of a Diels-Alder crosslinking reaction (see Figure 2).[19, 24] The two components are mixed together to afford a binary organic glass with an approximately 1:1 ratio of crosslinking moieties, and a relatively low initial T_g, ~ 75 ˚C. The crosslinking reaction is thermally activated, such that low-temperature (~65 ˚C) annealing can tune the T_g before poling, and during poling it can dramatically increase the T_g of the material, up to 160 ˚C or higher, through thermal ramping under the applied field. Initial studies suggest the resulting thermoset plastic material can exhibit large r_{33} values, in excess of 300 pm/V at 1310 nm, while also affording excellent thermal stability with no relaxation at 85 ˚C under inert conditions.[1, 19, 25] Herein we explore the shelf storage of commercially produced HLD material in non-encapsulated bulk EO devices under a variety of demanding thermal conditions relevant to Telecordia GR-468-CORE standards to understand the thermal stability potential of such materials for commercial applications. Furthermore, we also explore the shelf storage of poled HLD under various environmental conditions, up to and including the very aggressive damp heat condition, 85 ˚C / 85 % relative humidity (%RH), to understand the environmental sensitivity of HLD. In so doing, we deconvolute the relative contributions of thermal relaxation (reduction in $\langle\cos^3\theta\rangle$) and chemical degradation (reduction in ρ_N) to the observed overall changes in r_{33} and to help define encapsulation and packaging requirements for devices utilizing HLD.

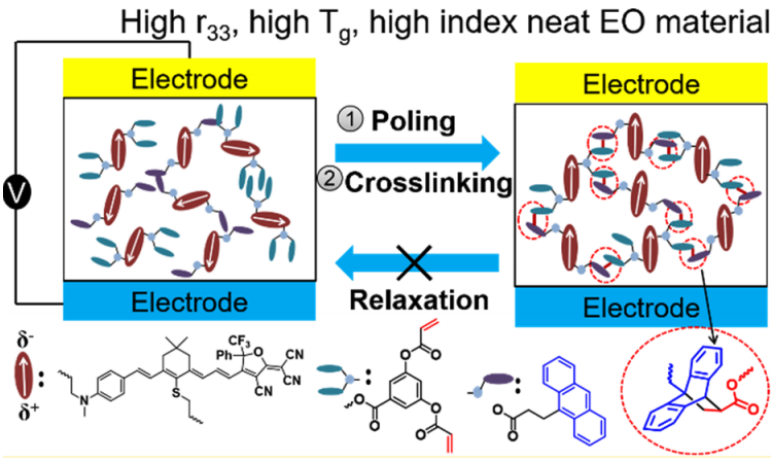

Figure 2. Schematic showing the structure and mechanism of the HLD OEO material system, capable of undergoing crosslinking during poling to afford increased thermal stability. Figure originally published in *Chemistry of Materials*.[19]

3. METHODOLOGY

The shelf storage thermal and environmental stability of the OEO materials was studied in non-encapsulated bulk film parallel plate capacitor devices, as shown in Figure 3, consisting of an ITO-on-glass bottom electrode, a charge barrier layer (CBL), an OEO active layer, and a sputter-deposited gold top electrode, with narrow gauge electrical wires attached via high temperature silver paint (Ted Pella, Inc. #16301). For each condition studied, several devices were prepared and each of their thicknesses (~1 μm) estimated by averaging the results of several optical profilometry measurements over multiple spots. Samples were electric field poled using a custom built, *in-situ* pole and probe simple reflection ellipsometric apparatus,[26] which allows application of a DC electric poling field (E_{pole}) and an 8 kHz AC modulating field (E_{ac}), while simultaneously measuring the leakage current (I_{dc}), effective poling voltage (E_{eff}), and the intensities of the unmodulated (I_c) and modulated (I_m, via lock-in amplifier) 1310 nm laser intensity, all under a nitrogen-enriched atmosphere. Samples are heated and cooled on an aluminum block stage to which the sample and a thermocouple reference are vacuum mounted. The 1310 nm laser is passed through a polarization controller with a Soleil-Babinet compensator, and then transmitted through the glass, ITO, CBL, and OEO material, reflected off the gold electrode at a 45˚ angle, and transmitted back out of the sample, through a polarization analyzer and collected by a photodiode.[26, 27] The ratio of the I_m signal to the I_c signal is proportional to the r_{33} response of the sample, allowing *in-situ* monitoring of the poling process. For crosslinked materials, such poling includes stepwise thermal ramps using previously optimized procedures to produce highly crosslinked materials.[19] After cooling and removing E_{pole}, but retaining E_{ac}, a sweep of the Soleil-Babinet compensator allows collection of the full I_m and I_c sinusoidal curves, and fitting those curves allows extracting accurate amplitudes, whose ratio allows calculation of the sample r_{33}.[27] For each sample the measurement is repeated in at least 3 spots and the average reported. For each set of experiments, after initial poling, parallel plate samples were assigned into groups of at least 3 devices for different exposure conditions to produce similar r_{33} distributions to that of the whole set.

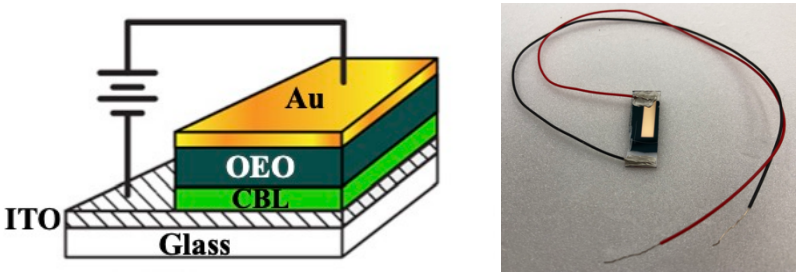

Figure 3. Schematic (left) and picture (right) showing the structure of a bulk film parallel plate capacitor OEO device.

For the bulk of our studies, HLD parallel plate capacitor devices utilized a 20 nm electron-beam evaporated titanium oxide (TiO_2) CBL and an applied E_{pole} of 75 V/μm. The standardized poling and crosslinking procedure consisted of:

1. heating the sample to 36 ˚C and applying the poling voltage gradually in seven steps of 10 V/μm, followed by a single step of 5 V/μm, to reach 75 V/μm;
2. heating the sample at ~10 ˚C/min to an initial poling temperature of 90-95 ˚C and holding for 10 min;
3. heating the sample an additional 10 ˚C and holding for another 10 min;
4. repeating step 3) until a temperature of 150-155 ˚C is reached;
5. turning off the heat and allowing the sample to cool to ~130-135 ˚C;
6. turning on active cooling and rapidly cooling to 35 ˚C.

The average E_{eff} sustained across the devices during the period from ~90 ˚C until rapid cooling was initiated was generally ~50-55 V/μm.

In addition to parallel plate devices, some studies utilized OEO films on glass, both ~1 μm thick (to match parallel plate thicknesses) and ~300 nm thick (to obtain measurable optical densities) to monitor chemical/environmental degradation of the OEO material. Independent studies indicated a negligible effect on chemical/environmental stability from

crosslinking, hence these films were only subjected to a standard pre-crosslinking step (65 ˚C /3 hrs under vacuum) before measurement of the UV-visible-NIR absorption spectra (300-1100 nm, Shimadzu UV-1601 spectrophotometer).

Vacuum ovens were plumbed with gas inlets (2 standard liters per minute laboratory N_2 or compressed air passed through anhydrous calcium sulfate) and temperatures monitored via external probe thermometers to establish stable temperatures at specified settings. Elevated humidity studies were performed in a BMT USA Climacell EVO 111 Climate Chamber. All samples were re-measured immediately before start of the experiment (t_0) and at regular intervals thereafter. Samples were removed from ovens/Climacell and allowed to cool rapidly to room temperature in ambient laboratory conditions, without protection from water and/or oxygen, before measuring at room temperature. In accordance with Telecordia GR-468-CORE standards, elevated temperature shelf storage studies were performed for 2000 hrs, while elevated humidity studies were performed for 500 hrs, with the exception of our initial ranging study.

4. RESULTS

For our first systematic investigation of HLD thermal and environmental stability, we examined the long-term (2000 hr) shelf storage stability of poled HLD at 85 ˚C under three different environmental conditions: N_2 (inert), laboratory air (ambient), and 85 %RH (damp heat) (Figure 4), with three unencapsulated samples under each condition. The samples stored in inert conditions showed no loss of r_{33} over the entire 2000 hrs, indicating that there is no reduction in ρ_N (no chemical degradation) or $\langle\cos^3\theta\rangle$ (no relaxation of orientational order) under these conditions. This is in distinct contrast to conventional guest-host OEO systems, where there is generally a significant (~20%) initial loss of r_{33} ('burn-in'), presumably due to loss of $\langle\cos^3\theta\rangle$, even if the T_g is significantly above 85 ˚C.[23] There is, however, significant loss of r_{33} over 2000 hrs for the ambient and damp heat samples (~33% and ~66%, respectively), which can be attributed solely to a reduction in ρ_N (chemical degradation), based on the results for the inert samples. This conclusion is supported by the change in UV-visible-NIR absorption properties of a thin film of HLD on glass subjected to the same 85 ˚C/85 %RH conditions (Figure 7). The change in r_{33} for the HLD 85 ˚C/Air and 85 ˚C/85 %RH devices, as well as the change in λ_{max} for the HLD thin film under 85 ˚C/85 %RH, were fit to a stretched exponential function (KWW model),

$$\frac{r(t)}{r_0} = e^{-\left(\frac{t}{\tau_K}\right)^{\beta_K}} \quad (2)$$

which is used for quasi-first order kinetics in amorphous systems with a distribution of processes and/or rate constants.[28, 29] The parameters for the fits are listed in Table 1. While the τ_K time constant (time to decrease by a factor of *e*) for the UV-visible-NIR data is substantially smaller (~ 41%) than for the r_{33} data under the same conditions, this is likely due to differences in sample geometry, i.e. the gold top electrode is probably slowing the rate of degradation in devices compared to the open surface of the thin film. Comparing the τ_K for r_{33} data between the two conditions that experienced degradation, the ~50% smaller time constant for the damp heat condition aligns well with expectations and observations.

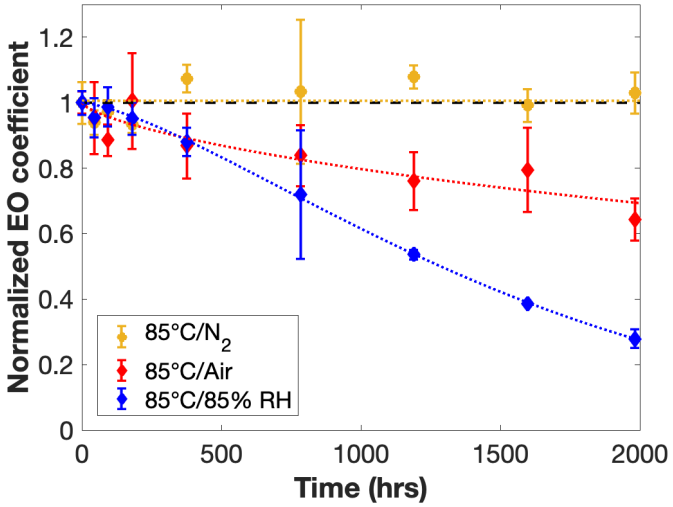

Figure 4. Long term shelf-storage stability of HLD parallel plate capacitor devices at 85 ˚C under various environmental conditions.

Table 1. Stretched exponential fit parameters for non-encapsulated HLD samples under 85 ˚C/Air and 85 ˚C/85 %RH.

Condition	Parameter	R^2	τ_K (hrs)	β_K
85 ˚C/Air	r_{33}	0.834	8490	0.69
85 ˚C/85 %RH	r_{33}	0.997	1670	1.41
85 ˚C/85 %RH	λ_{max}	0.965	989	1.04

Next, we built upon our initial results by examining the long-term shelf storage of HLD devices under N_2 at a variety of different temperatures, from 85 ˚C up to 135 ˚C (Figure 5). At temperatures above 85 ˚C, HLD shows a small initial reduction in r_{33} (burn-in), followed by relatively flat response. For the 105 ˚C condition, the best fit (R^2 = 0.75) was obtained with an exponential burn-in model, described by

$$\frac{r(t)}{r_0} = \frac{r_{eq}}{r_0} + \frac{(r_0 - r_{eq})}{r_0} e^{-b \cdot t} \qquad (3)$$

with r_{eq}/r_0 = 0.94. Attempting to fit with a stretched exponential yielded a significantly worse fit (R^2 = 0.60), however it also suggested a nearly indefinite lifetime after the initial burn-in, consistent with the exponential burn-in model. At higher temperatures, a stretched exponential yielded the best fit, with τ_K time constants of 4.17 x10^7 hrs at 120 ˚C (β_K = 0.18, R^2 = 0.89) and 4.65 x 10^4 hrs at 135 ˚C (β_K = 0.24, R^2 = 0.76). We note that there was a brief interruption (~ 3 hrs) to the flow of N_2 around 1600 hrs for the 135 ˚C condition which may have negatively impacted device performance thereafter. While we do not currently have thin film UV-visible-NIR data under these conditions, such data at 150 ˚C under N_2, which shows only mild degradation, suggests that most of this loss in r_{33} is likely attributable primarily to a reduction in $\langle\cos^3\theta\rangle$, and not loss of ρ_N. Regardless, the essentially infinite lifetime for HLD at 85 ˚C (100% of initial r_{33}) and 105 ˚C (94% of initial r_{33} after burn-in), and the very high τ_K of > 4500 years at 120 ˚C (~87% of initial r_{33} after burn-in) and τ_K ~5 years at 135 ˚C (~70% of initial r_{33} after burn-in) suggest that HLD is extremely thermally stable under inert conditions even at very high temperatures. This in turn suggests that hermetically sealed devices containing HLD should be sufficiently stable to permit long-term operation up to 120 ˚C without significant loss of performance, after the initial burn-in; we extrapolate a time to 80% (t_{80}) post-burn-in of 9.32 x 10^4 hrs (11 years) under these conditions. These results represent a significant improvement in maximum temperature for long-term stability versus

prior commercial OEO materials[20] capable of passing a 2000 hr/85°C test such as M3, while also exhibiting a much greater electro-optic response.

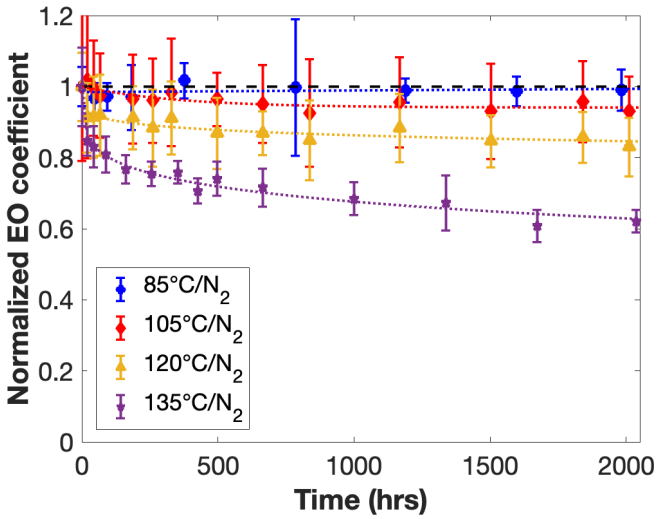

Figure 5. Long term shelf-storage stability of HLD parallel plate capacitor devices under N_2 at various temperatures.

While HLD is clearly quite stable under inert conditions, hermetic sealing is a significant added expense and constraint on device design, and thus it is desirable to avoid such a limitation if possible. To investigate that possibility, and characterize the sensitivity of HLD to moisture, we performed a series of experiments investigating the shelf storage of HLD devices at 85 %RH (in air) at a variety of temperatures from 35 ˚C to 85 ˚C (Figure 6). As all of these temperatures are insufficient to cause loss of $\langle\cos^3\theta\rangle$ in crosslinked HLD films, any loss of r_{33} can be conclusively assigned to loss of ρ_N (chemical degradation). At 35 ˚C and 55 ˚C, we saw no degradation in r_{33} (within experimental error) within the 500 hr experiment. At 70 ˚C, we saw only very minor degradation within the 500 hr experiment called for by Telecordia GR-468-CORE standards (black dashed vertical line), but continued the experiment in order to gain sufficient data to obtain a quality fit. The 70 ˚C data was fit with a stretched exponential, as for the previously collected 85 ˚C data, and yielded a τ_K of 1920 hrs ($\beta_K = 2.03$, $R^2 = 0.80$).

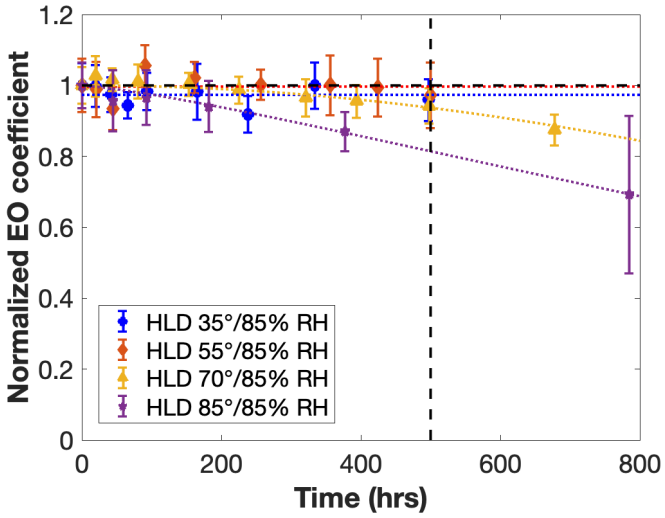

Figure 6. Shelf-storage stability of HLD parallel plate capacitor devices under 85 %RH (in air) at various temperatures.

To verify the chemical degradation of HLD under elevated humidity and temperature, we also examined the UV-visible-NIR absorption of thin films (Figure 7). As for the devices, we saw no degradation of HLD at 35 ˚C/85 %RH, which gives confidence for handling and processing the material under ambient laboratory conditions in even the most humid of locales. At 55 ˚C, interestingly, while we did not see degradation, we did see an apparent change in morphology as the absorption peak at 775 nm decreased, but the shoulder at 930 nm strengthened, pushing absorption more into the red. At 70 ˚C, as well as at 85 ˚C, we do see clear degradation, but the magnitude of the degradation is not excessive. Both 70 ˚C and 85 ˚C absorption data were well-fit by a linear model, as makes sense for a steady-state process at a surface, with slopes of -3.8 x 10^{-4} hr^{-1} at 70 °C and -8.4 x 10^{-4} hr^{-1} at 85 °C. The factor of 2.21 difference between these two rates, at a temperature difference of 15 ˚C, matches well with the 'rule of thumb' for Arrhenius behavior: a factor of 2 increase in rate for every 10 ˚C. This, combined with the relatively sharp transition from no reactivity (55 ˚C) to onset of degradation (70 ˚C), suggests there may be a specific mechanism for chemical degradation of HLD through reaction with water. This suggests that if the mechanism can be identified, it might be possible to alter the structure to prevent such a reaction and improve the environmental stability of future materials. Regardless, the relatively moderate sensitivity of HLD to even the aggressive damp heat conditions, as compared to OLEDs, suggests that modest barriers, on the order of 10^{-4} g/m^2day water vapor transmission rate (WVTR), may be sufficient to enable long term stability under such conditions.

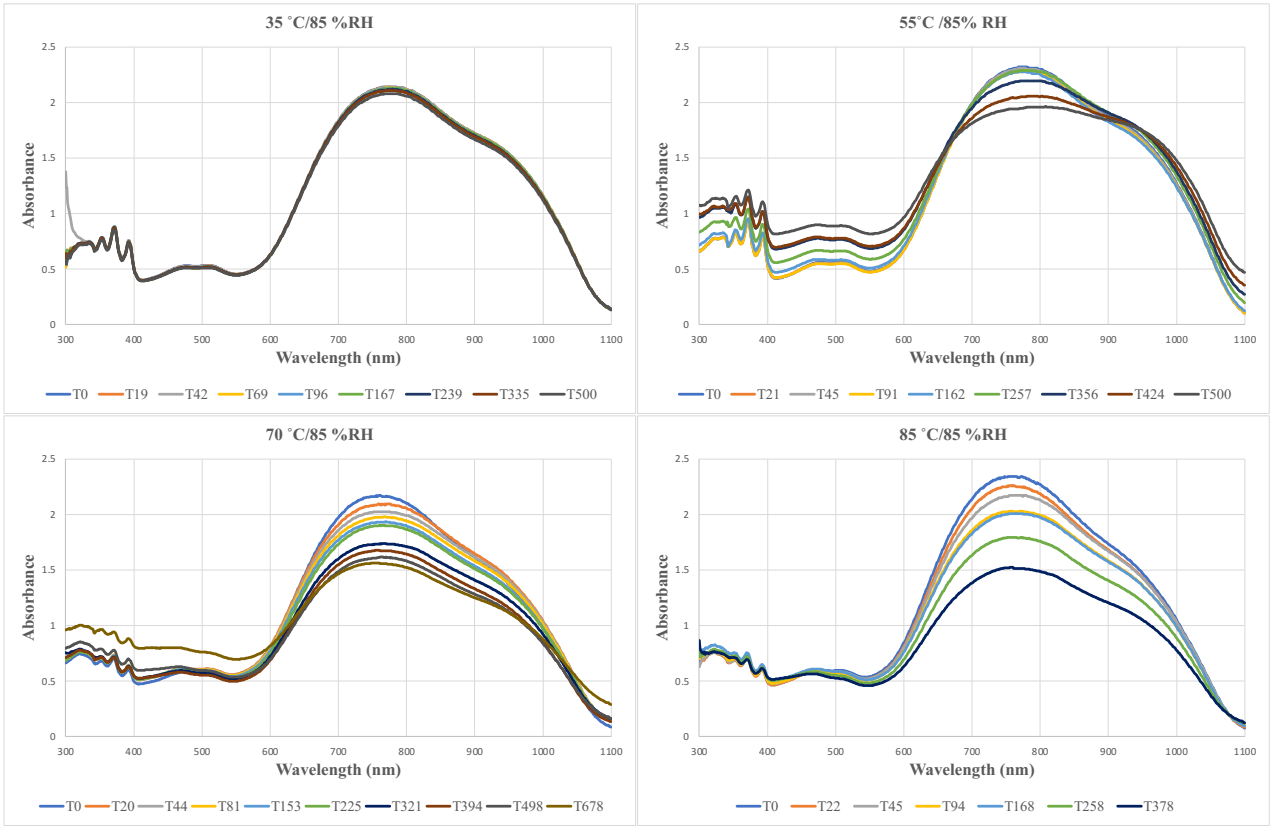

Figure 7. Shelf-storage stability of HLD thin films on glass under 85 %RH at various temperatures, as demonstrated by UV-visible-NIR absorption spectra of the thin film.

The preceding HLD parallel plate capacitor device data was all obtained with devices with a TiO_2 CBL and poled with an applied E_{pole} of just 75 V/µm, as opposed to the practical maximum for such devices of ~100 V/µm, to ensure a good yield of devices for achieving sufficient statistics in the study. This limited the average r_{33} for these devices to 101.5 ± 25.5 pm/V. To demonstrate that these results are applicable for higher-performance HLD devices, we also prepared two devices on a 20 nm atomic layer deposited (ALD) zirconium oxide (ZrO_2) CBL. This high dielectric constant CBL more effectively suppresses the I_{dc} while maintaining a high E_{eff} across the OEO material, as compared to the TiO_2 CBL, especially at higher poling/crosslinking temperatures. The devices were poled with an E_{pole} of 75 V/µm and 100 V/µm, and maintained an average E_{eff} of ~55 V/µm and ~60 V/µm, respectively. These samples exhibited t_0 average r_{33}s of

275.5 ± 12.1 pm/V and 353.4 ± 10.1 pm/V, respectively. The samples were exposed to 105 ˚C/N_2 and 120 ˚C/N_2 shelf-storage, respectively (Figure 8). The r_{33} decay for the sample at 105 ˚C was fit with a stretched exponential model with a τ_K time constant of 8.92 x 10^8 hrs (β_K = 0.13, R^2 = 0.64). While the other HLD device data at 105˚C/N_2 was best fit with an exponential burn-in model, when it was fit with a stretched exponential model, it gave a similar τ_K of 9.67 x 10^8 hrs (β_K = 0.22, R^2 = 0.60), which is a good match given the limited statistics provided by comparing with a single sample. Similarly, the sample at 120 ˚C was fit with a stretched exponential with a τ_K time constant of 2.26 x10^6 hrs at 120 ˚C (β_K = 0.13, R^2 = 0.81), as compared to 4.17 x10^7 hrs at 120 ˚C (β_K = 0.24, R^2 = 0.89) for the rest of the HLD devices at 120 ˚C. These results give confidence that the stability statistics gleaned from moderately-poled HLD devices are directly applicable to high-performance HLD devices with r_{33}s ≥ 300 pm/V.

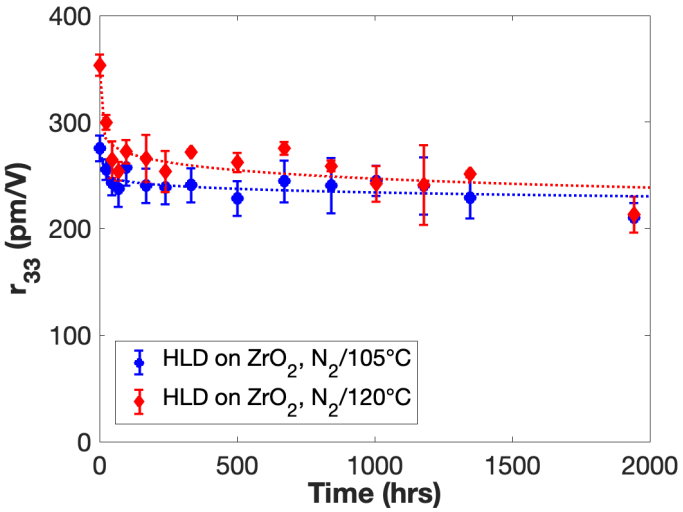

Figure 8. Long-term shelf-storage stability of individual HLD parallel plate capacitor devices on ZrO_2 CBL at 105 ˚C and 120 ˚C under N_2.

While the studies here have gone a long way towards demonstrating suitable stability of HLD for commercial applications, there remains more work to do. Shelf storage is of course just one measure of long-term stability, and necessary but not sufficient to prove operational stability. Sample geometry will be substantially different for nanophotonic devices as compared to the parallel plate capacitor devices studied here, which will likely change some of the detailed kinetics. Photochemical stability of OEO materials remains a major topic, as the optical powers in highly confined nanophotonic devices are extraordinarily high. Some early power handling results have been previously reported.[25] RF power handling of OEO materials is not well studied as of yet. All of these studies will depend on getting HLD into sufficient nanophotonic devices to enable the kind of high volume, long-term testing performed here. Our results here demonstrate that HLD possesses sufficient thermal and environmental stability to make such next steps worthwhile. They further demonstrate that due to excellent stability under high-temperature inert conditions, successfully deploying HLD and similar OEO materials for long-term stable devices is now a matter of packaging engineering and no longer limited by materials design.

5. CONCLUSIONS

In conclusion, we have examined the long-term shelf storage stability of the commercially available crosslinkable OEO material, HLD, under a variety of thermally and environmentally aggressive conditions in the absence of packaging or encapsulation and found it to have sufficient stability to enable commercial applications. HLD proved 100% stable at 85 ˚C under inert conditions (N_2), showing no chemical degradation or loss of order, in contrast to previous OEO materials. At higher temperatures under inert conditions, HLD shows only a small initial burn-in, attributed to modest reduction in orientational order, before relatively stable long-term performance; at 105 ˚C HLD retains ~94% of the initial r_{33} essentially indefinitely, while at 120 ˚C it retains ~ 87% of the initial performance after 2000 hrs, and exhibits a t_{80} of ~ 11 years assuming a 200 hr burn-in period. While HLD exhibits significant degradation under the aggressive 85 ˚C/85 %RH damp heat condition (in air), at 70 ˚C the degradation is significantly reduced, and at 35 ˚C and 55 ˚C no

degradation was seen at all. The kinetic data suggest a specific mechanism for water reacting with the constituent chromophores in HLD, which suggests the possibility to alter the structure and improve the stability of future materials. Additionally, the use of moderate barriers with WVTR ~ 10^{-4} g/m^{2}day may prove sufficient to enable the use of HLD without requiring full hermetic enclosures. Finally, we demonstrate that the kinetic results we obtained for HLD are directly applicable to very high-performance devices, with initial r_{33} values in excess of 300 pm/V.

ACKNOWLEDGEMENTS

The authors wish to thank Profs. Larry Dalton and Bruce Robinson (UW), and Dr. Wolfgang Heni (Polariton Technologies AG) for many helpful discussions and feedback. We also thank the Air Force Office of Scientific Research (FA9550-15-1-0319 and FA9550-19-1-0069), National Science Foundation (DMR-13030800, IIP-2036514), University of Washington, and Nonlinear Materials Corporation for financial support for this work.

FINANCIAL INTEREST DISCLOSURE

Drs. Johnson, Elder, Hammond, and O'Malley are employees of Nonlinear Materials Corporation, which provides materials and services related to organic electro-optic materials discussed in this work. Drs. Johnson, Elder, Hammond, and O'Malley, hold equity positions in Nonlinear Materials Corporation. Dr. Xu declares no competing financial interests.

REFERENCES

[1] L. E. Johnson, D. L. Elder, H. Xu *et al.*, [New paradigms in materials and devices for hybrid electro-optics and optical rectification], (2021).

[2] L. R. Dalton, P. Gunter, M. Jazbinsek *et al.*, [Organic Electro-Optics and Photonics] Cambridge University Press/Materials Research Society, Cambridge, UK(2015).

[3] L. R. Dalton, P. A. Sullivan, and D. H. Bale, "Electric Field Poled Organic Electro-optic Materials: State of the Art and Future Prospects," Chemical Reviews*,* 110(1), 25-55 (2010).

[4] H. Xu, D. L. Elder, L. E. Johnson *et al.*, "Design and synthesis of chromophores with enhanced electro-optic activities in both bulk and plasmonic–organic hybrid devices," Materials Horizons*,* 9, 261-270 (2022).

[5] H. Xu, D. L. Elder, L. E. Johnson *et al.*, "Electro-optic Activity in Excess of 1000 pm/V Achieved via Theory-guided Organic Chromophore Design," Advanced Materials*,* 33, 2104174 (2021).

[6] W. Heni, Y. Kutuvantavida, C. Haffner *et al.*, "Silicon–Organic and Plasmonic–Organic Hybrid Photonics," ACS Photonics*,* 4(7), 1576-1590 (2017).

[7] C. Kieninger, Y. Kutuvantavida, S. Wolf *et al.*, "Ultra-high electro-optic activity demonstrated in a silicon-organic hybrid modulator," Optica*,* 5, 739-748 (2018).

[8] C. Kieninger, C. Füllner, H. Zwickel *et al.*, "Silicon-organic hybrid (SOH) Mach-Zehnder modulators for 100 GBd PAM4 signaling with sub-1 dB phase-shifter loss," Optics Express*,* 28(17), (2020).

[9] S. Ummethala, J. N. Kemal, A. S. Alam *et al.*, "Hybrid electro-optic modulator combining silicon photonic slot waveguides with high-k radio-frequency slotlines," Optica*,* 8(4), (2021).

[10] W. Heni, C. Haffner, D. L. Elder *et al.*, "Nonlinearities of organic electro-optic materials in nanoscale slots and implications for the optimum modulator design," Optics Express*,* 25(3), 2627 (2017).

[11] B. H. Robinson, L. E. Johnson, D. L. Elder *et al.*, "Optimization of Plasmonic-Organic Hybrid Electro-Optics," Journal of Lightwave Technology*,* 36(21), 5036-5047 (2018).

[12] M. Ayata, Y. Fedoryshyn, W. Heni *et al.*, "Complete High-speed Plasmonic Modulator in a Single Metal Layer," Science*,* 358, 630-632 (2017).

[13] C. Haffner, D. Chelladurai, Y. Fedoryshyn *et al.*, "Low-loss plasmon-assisted electro-optic modulator," Nature*,* 556(7702), 483-486 (2018).

[14] A. A. Kashi, J. J. G. M. van der Tol, K. Williams *et al.*, "Electro-Optic Slot Waveguide Phase Modulator on the InP Membrane on Silicon Platform," IEEE Journal of Quantum Electronics*,* 10.1109/jqe.2020.3041943, 1-1 (2020).

[15] M. Burla, C. Hoessbacher, W. Heni *et al.*, "500 GHz plasmonic Mach-Zehnder modulator enabling sub-THz microwave photonics," APL Photonics, 4(5), (2019).
[16] W. Heni, Y. Fedoryshyn, B. Baeuerle *et al.*, "Plasmonic IQ modulators with attojoule per bit electrical energy consumption," Nature Communications, 10(1), (2019).
[17] U. Koch, C. Uhl, H. Hettrich *et al.*, "A monolithic bipolar CMOS electronic–plasmonic high-speed transmitter," Nature Electronics, 10.1038/s41928-020-0417-9, (2020).
[18] L. E. Johnson, D. L. Elder, A. A. Kocherzhenko *et al.*, "Poling-induced birefringence in OEO materials under nanoscale confinement," Organic and Hybrid Sensors and Bioelectronics XI, 10.1117/12.2321997, (2018).
[19] H. Xu, F. Liu, D. L. Elder *et al.*, "Ultrahigh Electro-Optic Coefficients, High Index of Refraction, and Long-Term Stability from Diels–Alder Cross-Linkable Binary Molecular Glasses," Chemistry of Materials, 32(4), 1408-1421 (2020).
[20] D. Jin, H. Chen, A. Barklund *et al.*, [EO polymer modulators reliability study], (2010).
[21] A. Rahim, A. Hermans, B. Wohlfeil *et al.*, "Taking silicon photonics modulators to a higher performance level: state-of-the-art and a review of new technologies," Advanced Photonics, 3(02), (2021).
[22] G.-W. Lu, J. Hong, F. Qiu *et al.*, "High-temperature-resistant silicon-polymer hybrid modulator operating at up to 200 Gbit s−1 for energy-efficient datacentres and harsh-environment applications," Nature Communications, 11(1), (2020).
[23] C. Kieninger, Y. Kutuvantavida, H. Miura *et al.*, "Demonstration of long-term thermally stable silicon-organic hybrid modulators at 85 °C," Optics Express, 26(21), (2018).
[24] Z. Shi, J. Luo, S. Huang *et al.*, "Reinforced Site Isolation Leading to Remarkable Thermal Stability and High Electrooptic Activities in Cross-Linked Nonlinear Optical Dendrimers," Chemistry of Materials, 20(20), 6372-6377 (2008).
[25] C. Hoessbacher, P. Habegger, M. Destraz *et al.*, [Plasmonic-Organic-Hybrid (POH) Modulators - a Powerful Platform for Next-Generation Integrated Circuits], (2021).
[26] B. C. Olbricht, P. A. Sullivan, G.-A. Wen *et al.*, "Laser-Assisted Poling of Binary Chromophore Materials†," The Journal of Physical Chemistry C, 112(21), 7983-7988 (2008).
[27] Y. Shuto, and M. Amano, "Reflection measurement technique of electro-optic coefficients in lithium niobate crystals and poled polymer films," Journal of Applied Physics, 77(9), 4632-4638 (1995).
[28] L. E. Benatar, D. Redfield, and R. H. Bube, "Interpretation of the activation energy derived from a stretched-exponential description of defect density kinetics in hydrogenated amorphous silicon," Journal of Applied Physics, 73(12), 8659-8661 (1993).
[29] N. Rabiei, S. H. Amirshahi, and M. Haghighat Kish, "Description of physical aging kinetics of glassy polymers by interpretation of parameters of the Kohlrausch-Williams-Watts relaxation function via simulation," Physical Review E, 99(3), (2019).